Solid lipid nanoparticles of cholesteryl butyrate inhibit the proliferation of cancer cells in vitro and in vivo models.

UNIVERSITÀ DEGLI STUDI DI TORINO

Cholesteryl butyrate solid lipid nanoparticles inhibit the proliferation of cancer cells *in vitro* and *in vivo* models

[1]R Minelli, [2]S Occhipinti, [3]C L Gigliotti, [2]G Barrera, [4]P Gasco, [5]L Conti, [3]A Chiocchetti, [1]G P Zara, [1]R Fantozzi, [2]M Giovarelli, [3]U Dianzani and [1]C Dianzani

[1]Department of Drug Science and Technology - University of Turin, Torino, Italy.

[2]Department of Medicine and Experimental Oncology, University of Turin, Torino, Italy.

[3]Interdisciplinary Research Center of Autoimmune Diseases (IRCAD) and Department of Health Sciences, "A. Avogadro" University of Eastern Piedmont, Novara, Italy.

[4]Nanovector s.r.l. Torino, Italy.

[5]Molecular Biotechnology Center, University of Turin, Torino, Italy.

Running Title: Cholbut SLN inhibit cancer cell proliferation.

Word Number: 6791; Figure Number: 9; Table number 1

Corresponding author: Dr. Chiara Dianzani, Tel:+39-011-6707690, Fax:+39-011-6707688, e-mail: chiara.dianzani@unito.it.

This article has been accepted for publication and undergone full peer review but has not been through the copyediting, typesetting, pagination and proofreading process, which may lead to differences between this version and the Version of Record. Please cite this article as doi: 10.1111/bph.12255

BACKGROUND AND PURPOSE

Cholesteryl butyrate solid lipid nanoparticles (cholbut SLN) can be a delivery system for the anti-cancer drug butyrate. We have previously shown that they inhibit adhesion of polymorphonuclear and tumor cells to endothelial cells and migration of tumor cells, suggesting that they may act as anti-inflammatory and antitumor agents. The aim of the research was to evaluate the activity of cholbut SLN on tumor cell growth using *in vitro* and *in vivo* models.

EXPERIMENTAL APPROACH

Cholbut SLN were incubated with four tumor cell lines, and cell growth was analysed by assessing viability, clonogenic capacity and cell cycle. The effect on signalling was evaluated by western blot analysis of Akt expression. The *in vivo* anti-tumor activity was assessed using two models of PC-3 cell xenografts in SCID/beige mice.

KEY RESULTS

Cholbut SLN inhibited tumor cell line viability, clonogenic activity, Akt phosphorylation, and cell cycle progression. Mice were injected i.v. with PC3-Luc cells and treated with cholbut SLN. In vivo optical imaging and histological analysis showed that no metastases were detected in the lungs of the treated mice. Mice were injected s.c. with PC-3 cells and treated with cholbut SLN when the tumor diameter reached 2 mm. Analysis of the tumor dimensions showed that treatment with cholbut SLN substantially delayed tumor growth.

CONCLUSION AND IMPLICATIONS

These results demonstrated that cholbut SLN is effective in inhibiting tumor growth and suggest that this effect may partly involve inhibition of AKT phosphorylation, which adds another mechanism to the activity of this multifaceted drug.

Key words: Solid lipid nanoparticles, cholesteryl butyrate, clonogenic assay, tumor growth *in vivo*.

Abbreviations

Cholbut, cholesteryl butyrate; SLN, solid lipid nanoparticles; Cholbut SLN, Cholesteryl butyrate solid lipid nanoparticles; EPR, enhanced permeability and retention; FCS, fetal calf serum; HDACI, histone deacetylase inhibitor; HUVEC, human umbilical vein endothelial cell; MCT1, monocarboxylate transporter 1; Nabut, sodium butyrate; PBS, phosphate buffered saline; P-glycoprotein, Pgp; PMA, phorbol 12-myristate 13-acetate; SCFAs, short chain fatty acids; SMCT1, sodium coupled monocarboxylate transporter 1.

INTRODUCTION

Cytotoxic anticancer drugs display problems, such as poor specificity, high toxicity, and susceptibility to induce drug resistance, which substantially limit their use. Their conventional administration often leads to their extensive and indiscriminate binding to body tissues and serum proteins in a highly unpredictable manner, and only a small fraction of the drug actually reaches the tumor site (Ho Lun Wonget *et al*., 2007); this reduces their therapeutic efficacy and increases the systemic toxicity. Since the early 1990s, a number of solid lipid nanoparticles (SLN) or SLN-based systems have been successfully formulated and tested for the delivery of cytotoxic drugs (Ho Lun Wong *et al*., 2007). These are particles of submicron size (50-100 nm) intended to leak out of the blood vessels and accumulate within the tumor. In terms of drug stability, drug biodistribution, pharmacokinetics, and cancer activity, SLN formulations of anticancer agents have been shown to be superior to the corresponding free drug, and they are at least comparable to other drug carrier systems such as polymeric systems and liposomes. In many cases, nanoparticles also have the potential to bypass the multidrug resistance mechanisms that involve cell-surface pump proteins through their entry into the cells via endocytosis (Davis *et al*., 2008). Moreover, nanocarriers may preferentially concentrate in tumors, inflammatory sites, and antigen sampling sites by virtue of the enhanced permeability and retention (EPR) effect on the vasculature of these sites. Once biodegradable nanoparticles have accumulated at the target site, they can act as local drug depots depending on the make-up of the carrier, thus providing a source of continuous supply of encapsulated therapeutic compound(s) at the solid tumor site (Singh and Lillard 2009).

Butyrate has received close attention as a potential chemopreventive agent (Wolloski *et al*., 2001; Delzenne *et al.,* 2003), especially because *in vitro* exposure of tumor cells to this agent induces apoptosis, inhibits proliferation, and promotes differentiation (Kobayashi *et al*., 2003) in tumor cells derived from colorectal, breast, gastric, lung, brain, and pancreas cancers (Brioschi *et al*., 2008). Moreover, Sodium Butyrate (Nabut) has displayed some efficacy as an anti-tumor drug in phase I and phase II clinical trials, possibly through its Histone Deacetylase Inhibitor (HDACI) activity (Minucci *et al.*, 2006). However, its short half-life limits its clinical use (Pellizzaro *et al.*, 1999), and maintenance of therapeutic concentrations requires a continuous parenteral administration. Moreover, compliance is further reduced by several adverse events, such as abdominal cramps, nausea, diarrhoea, anaemia, headache, and strong odour.

The warm microemulsion method has been used to prepare Cholesteryl butyrate (cholbut) SLN with an average diameter around 80 nm, to be used as a pro-drug of butyric acid (Gasco, 2004; Matsumura and

Kataoka, 2009). They had negative zeta potential, high enough in modulus to prevent their aggregation and to obtain stable nanoparticle dispersions. They were rapidly internalized and displayed an antitumor effect greater than that of butyrate in several tumor cell lines (Salomone *et al*., 2001; Serpe *et al*., 2004; Minelli *et al*., 2012).

In previous works, we showed that cholbut SLN inhibited adhesion to human umbilical vein endothelial cells (HUVEC) and migration of several types, including several cancer cell lines (Dianzani *et al*., 2006, Minelli *et al*., 2012). The anti-adhesive effect was exerted by acting on both HUVEC and the cancer cells. We therefore suggested that cholbut SLN may be used as antitumor agents.

The aim of the research reported here was to extend these analyses by assessing the anti-proliferative potential of cholbut SLN on tumor cell lines and to investigate whether the Akt pathway can be involved in determining cholbut SLN effects. Indeed. activation of Akt by phosphorylation plays an important role in a variety of malignancies such as colon, breast, prostate and non-small cell lung cancer, where it is involved in mediating a variety of biological responses, including cell growth, proliferation and survival (Roy *et al*., 2002; Asano *et al*., 2004).

The results showed that cholbut SLN strikingly decreased viability and proliferation of the colon cancer cell lines HT29, HCT15, and HCT116, and the prostate cancer cell line PC-3, by acting in a concentration- and time-dependent manner and with activity higher than that of the free butyrate. These effects may involve inhibition of the Akt pathway and cell cycle arrest in the S and G2/M phase. Moreover, cholbut SLN inhibited dissemination and growth of cancer cells *in vivo*, which supports the efficacy of cholbut SLN in anti-cancer therapy.

METHODS

Preparation of cholbut SLN and sodium butyrate solutions

Cholbut SLN were prepared by warm microemulsion (μE) method reported elsewhere (Minelli *et al*., 2012) and described in PATENT WO0030620. Briefly, warm oil-in-water μE was prepared by melting cholesterylbutyrate (Asia Talent Chemical, Shenzen China), Epikuron 200 (Cargill, Milan, Italy) at 85°C as lipid phase, and then adding external water phase containing Sodium Glycocholate (PCA, Basaluzzo, Italy). Since melting point of cholesteryl butyrate is 98°C, 2-phenylethanol (Sigma Aldrich, Milan, Italy) was used in process to help melting step with goal to add its preservative efficacy in final product (final concentration about 0,25% w/V). After stirring, obtained clear μE was dispersed in cold water (2/4 °C) with a dispersion ratio μE /water of 1:10. Cholbut SLN dispersion was then washed by tangential flow filtration (TFF) using Vivaflow 50 membrane (Sartorius Stedim Biotech GmbH, RC,

Cut-off 100,000 Da). For in vivo experiments, further concentration of cholbut SLN was performed by TFF, up to obtain a concentration more than doubled comparing with original. Finally all aqueous dispersions of cholbut SLN, for *in vitro* or *in vivo* experiments, were sterilized by filtration at 0.2 μm before use, and no loss of cholbut contents was showed by HPLC analysis.

In Cholbut SLN, the whole lipid matrix itself acts as a prodrug of butyrate. Since the loading efficiency of these preparations can't be properly defined, compared to the usual situation in which a drug is incorporated in the SLN carrier, high recovery of the hydrophobic prodrug matrix was taken as the reference parameter for quality control. This always detected a minimal concentration reduction during 4 washing steps, possibly due to adsorption to the membranes, since no cholbut was found in the washing water. Moreover, no loss of either cholbut SLN or free butyrate was detected after the sterilizing filtration step.

Characterization of cholbut SLN formulations was performed by Dynamic Light Scattering (DLS, Malvern Zetasizer - Nano ZS), HPLC-UV analysis (Agilent 1260), Field Emission Scanning Electron Microscopy (FeSEM–ZEISS, SUPRA 40, GEMINI column, SMARTSEM software) and Laser Doppler Micro-electrophoresis (LDME, Malvern Zetasizer-Nano ZS). Gel Permeation Chromatography (GPC) analysis have been performed for further studying size distribution, using a glass column (1 cm diameter, 25 cm height) filled with Sepharose CL-4B (Sigma Aldrich, Milan, Italy) loaded with 1 mL cholbut SLN and eluted with PBS (pH 7.4).

Sodium butyrate (Nabut) solutions were freshly prepared in sterile water before each experiment, at a concentration of 5 M.

Cell culture

HT29, HCT15 and HCT116 cells from human colon adenocarcinoma were obtained from American Type Culture Collection (Manassas, VA), PC-3 from human prostate carcinoma were gifted by Dr. Pili (Roswell Park Cancer Institute, Buffalo, USA). Cholbut SLN was produced by Dr. Gasco (Nanovector s.r.l. Torino, Italy). The human tumor cell lines were grown in culture dishes as a monolayer in RPMI 1640 medium plus 10% FCS, 100 $U \cdot mL^{-1}$ penicillin, 100 $mg \cdot mL^{-1}$ streptomycin, at 37°C in a 5% CO_2 humidified atmosphere.

PC-3Luc cells were constructed by stably transfecting PC-3 cells with luciferase construct, as previously described (Loberg et al., 2006).

Cell viability assay

The effect of cholbut SLN on cell growth and survival was assessed by the MTT assay. Briefly, cells were normalized at 800 cells per 100 µl in 96-well plates. After an overnight incubation, the medium was replaced with 100 µl of culture medium with from 50 to 300 µM cholbut SLN or NaBut. After 24, 48 and 72 h of incubation, viable cells were measured, by 2,3-bis[2-methoxy-4-nitro-5sulphophenyl]-2H-tetrazolium-5carboxanilide (Sigma-Aldrich, Milan, Italy) inner salt reagent, at UV 490 nm, as described by the manufacturer's protocol. In some experiments, cholbut SLN or NaBut from 50 to 300 µM was refilled every 24 h. The UV readings of controls (i.e., cells that had received no drug) were normalized to 100%, and the readings from cholbut SLN-treated cells were expressed as % of controls. Eight replicate wells were used to determine each data point and three different experiments were performed.

Colony-forming assay

Cells (800 per well) were seeded into 6-well plates and treated with the compounds. The medium was changed after 72 h and cells were cultured for additional 10 days. Subsequently, cells were fixed and stained with a solution of 90% crystal violet (Sigma-Aldrich) and 10% methanol. Colonies were then photographed and counted with a Gel Doc equipment (Bio-Rad Laboratories, Milan, Italy).

Cell cycle analysis

PC-3 cells ($1.5x10^7$) were seeded and treated with titrated doses (50 to 300 µM) of cholbut SLN. After 24, 48 and 72 h, adherent and non-adherent cells were collected, washed in 1 x PBS (phosphate buffered saline) and fixed in 75% ice cold ethanol and subsequently resuspended in a buffer containing 0.02 $mg \cdot mL^{-1}$ RNase A (Worthington Biochemical Corporation, Lakewood, NJ), 0.05 $mg \cdot mL^{-1}$ propidium iodide (Sigma-Aldrich), 0.2% v/v Nonidet P-40 (Sigma-Aldrich), 0.1% w/v sodium citrate (Sigma-Aldrich). Samples were acquired with a FACSCalibur cytometer (Becton Dickinson) and analyzed with the software FlowJo v8.6.3 (Becton Dickinson).

In some experiments (n=3), cholbut SLN (50-300 µM) was refilled every 24 h.

Western blot analysis

Cells, treated or not with 0.1 mM cholbut SLN for 8-48 h were exposed to 0.01 µM Phorbol 12-myristate 13-acetate (PMA) (Sigma-Aldrich) for 10 min to stimulate Akt activation. They were then lysed in a buffer composed of 50 mM Tris-HCl pH 7.4, 150 mM NaCl, 5 mM EDTA, 1% NP40, phosphatase and protease inhibitor cocktail (Sigma-Aldrich). Cell lysates were then cleared from insoluble fractions through high speed centrifugation, and protein concentrations were determined with

a commercial kit (Bio-Rad Laboratories). Proteins (40 μg/lane) were loaded on 10% SDS PAGE gels and, after electrophoresis, transferred onto nitrocellulose membranes. These were blocked by incubation for 1 h at room temperature with 5% nonfat milk dissolved in TBS Tween 20. The membranes were then probed overnight with primary antibodies and, after 3 washes, incubated for 1 h with HRP-conjugated secondary antibodies (Bio-Rad Laboratories). Bands were detected by chemiluminescence, and densitometric analysis was performed with the Multi-Analyst software (version 1.1, Bio-Rad Laboratories).

Tumor growth in vivo

Female 4–5 week-old SCID/Beige mice (Charles River Laboratories, Milan, Italy) were housed under pathogen-free conditions. The mice were manipulated and housed according to protocols approved by the Turin University Bioethical Committee and the Italian Ministry of Health.

In the metastasis experiments, mice were injected in the tail vein with stably expressing firefly luciferase PC-3 cells (PC-3luc, $1x10^6$ per mouse) and monitored weekly for pulmonary metastases by *in vivo* optical imaging.

In the tumor growth experiment, mice were injected sub-cutaneously in the left flank with $2x10^6$ PC-3 cells. Tumor size was weekly quantified in two dimensions using calipers. Tumor volume was calculated as follows: tumor volume (mm^3)=$Dxd^2/2$, where D represents the largest cross sectional diameter (mm) of the tumor, and d the cross sectional diameter (mm) at right angles to D.

In each experiment, the mice were treated every 2 days with i.p. injection of 220 $mM \cdot Kg^{-1}$ cholbut SLN, or PBS as control.

In vivo optical imaging

At 0, 7, 14, and 21 days after tumor cell injection, mice (n=9) were injected i.p. with 150 $mg \cdot Kg^{-1}$ luciferin (PerkinElmer, Waltham, MA) in sterile PBS. They were then placed in the IVIS 200 (PerkinElmer) induction chamber and subjected to inhalational isoflurane anesthesia (Abbott, Abbott Park, IL) at 2.5% with 1 $L \cdot min^{-1}$ flow of oxygen. After 10 min, the mice were placed on the heated imaging platform of the IVIS 200 imaging station, with inhalational isoflurane anesthesia during the imaging procedure. White light and luciferase activity images were acquired with a 25 s exposure. Following imaging, the mice were removed from the imaging stage and allowed to recover from anesthesia and returned to their original housing. Images were analyzed with the Living Image software (PerkinElmer). The luminescent signal was quantified as the average radiance ($p/s/cm^2/sr$) measured in

regions of interest (ROIs) drawn in the lungs.

Histopathological analysis

The lungs were harvested at necropsy and fixed in 10% formalin. The fixed samples were then embedded in paraffin and four non-sequential serial sections per animal were obtained. The sections were stained with hematoxylin/eosin and analyzed for the presence of metastases by light microscopy.

Data analysis

Data are shown as mean±SEM. Statistical analyses were performed with GraphPad Prism 3.0 software (La Jolla, CA, USA) using one-way ANOVA and Dunnett's test. Values of $P < 0.05$ were considered statistically significant.

Materials

Cholbut SLN was produced by Dr Gasco (Nanovector s.r.l. Turin, Italy). Fetal calf serum (FCS, endotoxin tested) was from Hyclone Laboratories (Milan, Italy). Trypsin was from Difco Laboratories (Milan, Italy). M199, RPMI 1640, PMA, sodium butyrate and β-actin (A-1978) were purchased from Sigma-Aldrich. P-Akt was purchased from Santa Cruz Biotechnology (Santa Cruz, CA).

RESULTS

Cholbut SLN characterization

Table 1 shows the average diameter (Zave) and polydispersity index (PI) of cholbut SLN, evaluated by DLS, and the chemical composition, evaluated by HPLC-UV analysis, at different steps of the preparation process. Zeta Potential of cholbut SLN, evaluated by LDME after the final filtration step, was - 49.5 mV (Figure 1). FeSEM analysis confirmed the size and spherical morphology of cholbut SLN (Figure 2). GPC analysis (data not showed) evidenced the presence of two main populations of particles ($Zave_{39\%}$ = 183,75 nm, $Zave_{61\%}$ = 39,06 nm, $Zave_{max}$ = 227 nm), which could explain the relatively high value of polydispersity index.

Cholbut SLN inhibit tumor cell growth

Initially, we compared the ability of cholbut SLN and free NaBut to inhibit the growth of HT29, HCT116, HCT15 and PC-3 cells. Cells were cultured in the presence and absence of titrated amounts (50 μM-0.3 mM) of each compound for 24-48-72 h, and the amount of viable cells was then assessed by the MTT assay. In some experiments, each compound was refilled every 24 h. Figure 3 shows the inhibition of cell proliferation induced by cholbut SLN and by NaBut. The effect was concentration- and time-dependent with some differences between the four cell lines and the two substances. NaBut was active only in certain conditions. The most responsive cell line was HCT116, but only at the highest compound concentration and after 48-72 h of treatment, showing about 45% of growth inhibition at both these times. HCT15, HT29 and PC-3 were only weakly sensitive since they showed a respective growth inhibition of <5%, 15%, 20% at 48h, and 15%, 30%, 20% at 72 h. NaBut effectiveness increased in the refilling experiments, especially in HCT116 and PC-3, with a maximal inhibition of 35-50% obtained at 100 and 300 μM after 72 h for PC-3 and 35-60% for HCT116. By contrast, all cell lines were sensitive to cholbut SLN, especially in the refilling experiment, and the maximal inhibition reached approximately 55-80%. To investigate the possibility that cholesteryl esters may exert cell toxicity not related to NaBut, we evaluated the effect of similar SLN formulation, having cholesteryl palmitate as lipid matrix (50 μM-0.3 mM), on cell growth of the four tumor cell lines using the MTT assay. Results showed that cholesteryl palmitate SLN did not exert any effect on cell growth even at the highest concentrations (data not shown). These results are in agreement with our previous observations showing the ineffectiveness of cholesteryl palmitate SLN in inhibiting adhesion and migration of colon cancer cells (Minelli et al., 2011).

To validate these findings, clonogenic survival assays were performed. Cells were seeded into 6-well plates and treated with each compound. The culture medium was changed after 72 h, and cells were cultured for an additional 10 days in the absence of the compounds**.** The results were similar to those obtained with the MTT assay (Figure 4). Indeed, only HCT116 and PC-3 were partly sensitive to NaBut, whereas all cell lines were sensitive to cholbut SLN, whose maximal inhibition ranged 50-90%. The observation that the inhibition detected by the clonogenic assay was substantially higher than that detected by the MTT assay suggests that cells which were still viable after the cholbut SLN treatment in the MTT assay were severely damaged and unable to proliferate in the clonogenic assay.

To assess whether inhibition of cell proliferation induced by cholbut SLN affected cell cycle progression, we analyzed the cell cycle in PC-3 cells cultured in the presence and the absence of titrated amounts (50 - 300 µM) of cholbut SLN for 24-48-72 h (Figure 5a and 5b). Results showed that treatment with the highest concentration (300 µM) caused a significant accumulation of cells in the G2/M phase, but some effect was detected also at the lower doses. Experiments in which the compound was refilled every 24 h and the cell cycle analyzed after 48 and 72 h (Figure 5c and 5d) showed a substantial increase of cells in G2/M phase already detectable at the lowest compound dose, whereas the highest dose induced accumulation of cells in the SubG1 phase.

We then evaluated cell death in PC-3 cells refilled with cholbut SLN (50 - 300 µM) for 48-72 h by means of Annexin V/Propidium Iodide staining. Figure 6 shows that treatment with 300 µM of cholbut SLN caused substantial cell death since only 60% live cells were detected at 48 h, and this value decreased to 30% at 72 h. By contrast, the 50 µM and 0.1 mM doses were ineffective in cell death induction.

Cholbut SLN modulate Akt signaling

To investigate the mechanism of cholbut SLN-mediated inhibition of cell proliferation, we evaluated Akt phosphorylation, since the Akt signaling pathway is involved in the regulation of cell proliferation, apoptosis, adhesion, and migration (Kwiatkowska *et al*., 2011; Matsuoka *et al*., 2012). To this end, HCT15, HCT116, HT29 and PC-3 cells were incubated or not with 100 µM cholbut SLN for 8-48 h and then treated with 0.01 µM PMA for 10 min to induce Akt phosphorylation. Western blot analysis showed that Akt phosphorylation was induced by PMA in all cell lines (Figure 7), and was inhibited by cell treatment with cholbut SLN in a time-dependent manner.

In vivo experiments

To assess the effect of cholbut SLN *in vivo*, mice were injected i.v. with $1x10^6$ PC-3-Luc cells and treated every 2 days with i.p. injection of 220 $mM \cdot Kg^{-1}$ cholbut SLN (n=5) or PBS as control (n=4). The dose was chosen according to preliminary experiments that demonstrated that cholbut SLN did not induced any in vivo toxicity in mice upon delivery either p.o. or i.v. (oral $LD_{50} \geq 1000$ $mg \cdot kg^{-1}$; i.v. $LD_{50} \geq 400$ $mg \cdot kg^{-1}$; Minelli et al., 2011). At time 0, and 7, 14, and 21 days after cell injection, the mice were i.p. injected with luciferin and analyzed by *in vivo* optical imaging to evaluate the tumor cell growth in the lungs. Qualitative (8a) and quantitative (Figure 8b) analyses showed that a progressively increasing luminescent signal was present in the lungs of 3 out of 4 control mice, while no signal was detected in the lungs of the mice treated with cholbut SLN. To refine these data, histological analysis of the lungs was performed in the mice sacrificed at day 28. Results showed disseminated tumor foci in the lungs of the control mice (Figure 8c, left panel), while no metastases were detected in the lungs of the mice treated with cholbut SLN (Figure 8c, right panel).

To further assess the cholbut SLN effect on the tumor growth *in vivo*, mice were injected s.c. with PC-3 cells and treated with either cholbut SLN or PBS starting when the tumor diameter reached 2 mm. Analysis of tumor dimensions showed that treatment with cholbut SLN significantly delayed and reduced the tumor growth compared to that detected in the control mice (Figure 9). Meanwhile, there was no significant difference in body weight between the treated and the control group (data not shown), suggesting that the administered dose of cholbut SLN had no significant toxicity to the mice.

DISCUSSION AND CONCLUSION

Cancer progression is a multi-step process that enables tumor cells to avoid the growth checkpoints of the organism, giving rise to a primary tumor mass that may invade the surrounding tissues and even disperse far away, leading to metastases. If detected in the early stages, solid cancer is often locally circumscribed and can be treated successfully by surgical and radiotherapy removal of the primary tumor. The mortality of more than 90% of cancer patients is mostly due to the development of metastases (Hayot *et al*., 2006,). Cell movements through the tissues play a crucial role in cancer invasion and dissemination. Therefore, an effective anti-tumor therapy should be effective in inhibiting both the growth and invasiveness of tumor cells.

In an earlier work, we showed that cholbut SLN may have an effect in tumor cell dissemination because it inhibited adhesion of tumor cell lines to vascular endothelial cells and their migratory activity, which suggested that cholbut SLN may work as an anti-metastatic compound (Minelli *et al*.,

2012). The present work further strengthens findings on the anti-tumor effectiveness of cholbut SLN by showing its ability to inhibit cancer cell growth both *in vitro* and *in vivo*.

Our data show that cholbut SLN inhibited tumor cell growth *in vitro* at higher doses than those effective on tumor cell adhesion and migration. The effect was dose- and time-dependent and clearly more potent than that displayed by NaBut, which has been found to be ineffective on tumor cell adhesion and migration in our previous work. Moreover, NaBut is selectively effective in some tumor cell lines, whereas cholbut SLN were active on all cell lines tested. Wilson *et al*., 2010 demonstrated that cancer cell sensitivity to NaBut correlated with its capacity to inhibit HDAC activity. The cholbut SLN effect would be independent from HDAC inhibition because our previous work showed that these cholbut SLN doses do not inhibit HDAC (Minelli *et al*., 2012). Moreover, cholbut SLN was similarly effective in cell lines whose growth is either sensitive (HCT116) or resistant (HT29) to HDAC inhibitors (Wilson et al., 2010).

Inhibition of cell growth was due to cycle arrest in the G2/M or SubG1 phase and induction of significant cell death.

In our previous work, we showed that cholbut SLN inhibit the ERK and p38 pathways involved in cell growth, migration, and adhesion. Now, we extend those findings by showing that it inhibits the Akt pathway, too, which is overexpressed in a number of cancers, including colon, pancreatic, ovarian, and some steroid hormone-sensitive breast cancers (Roy *et al*., 2002; Asano *et al*., 2004). This effect is intriguing since the Akt pathway is critical for prostate cancer invasion (Shukla *et al*., 2007), promotes androgen-independent progression, and is essential for neuroendocrine differentiation of the prostate cancer (Li *et al*., 2007; Wu et al., 2007). Moreover, Akt phosphorylation correlates with cell growth, differentiation, and adhesion (Lai et al., 2010), as well as with the invasion grade, vessel infiltration, metastasis to lymph nodes, and tumor stage in human colon carcinomas (Itoh *et al*., 2002; Khaleghpour *et al*., 2004). These data indicate that cholbut SLN have an effect in the signalling machinery of tumor cells, but a wider analysis is needed to better depict these effects.

High concentrations of butyrate (about 2–3 mM) are present in the colon lumen. Since they reach pharmacological effectiveness, colon cancer cells can grow only upon development of escape mechanisms. Among these, a role seems to be played by the decrease of the intracellular concentration of butyrate through downregulation of monocarboxylate transporter 1 (MCT1) and sodium-coupled monocarboxylate transporter 1 (SMCT1) (Davis *et al*., 2008), which are involved in the transport of butyrate and other SCFA (short chain fatty acids) anions. Therefore, cholbut SLN may overcome this resistance by forcing butyrate uptake in the tumor cell through a transporter-independent mechanism.

Indeed, upon treatment with cholbut SLN, substantial uptake of butyrate is already detectable after 15 min, and it then persists inside the cell for several days (Brioschi et al., 2008; Minelli *et al*., 2012). Development of multidrug resistance in human tumors is one of the main obstacles to the success of cancer chemotherapy. This phenomenon is often associated with increased expression of the mdr1 gene, which encodes P-glycoprotein (Pgp). As an energy-dependent efflux pump, this protein is capable of extruding certain drugs from cells, leading to decreased drug concentrations within the cells and reduced efficacy of drugs (Stein *et al*., 1996). The human colon carcinoma cell lines HCT116 and HCT15 were selected in this work also because they express the Pgp-mediated type of multidrug resistance intrinsically. However, HCT15 displays a greater multidrug resistance than HCT116 (Iwahshi *et al*., 1991; Lee *et al*., 2010), which might explain the higher activity of NaBut on HCT116 than on HCT15. Therefore, the observation that chobut SLN similarly inhibited HC116 and HCT15 supports the hypothesis that they escape the transmembrane efflux pumps responsible for drug elimination.

The *in vivo* data support the *in vitro* data and show that cholbut SLN have significant antitumor activity against PC-3 by inhibiting local tumor growth after s.c. injection of the cell line. Moreover, it inhibited lung metastasis dissemination after i.v. injection of the cell line, which may involve the cholbut SLN effect on tumor cell adhesion, migration, and growth. In the light of these results, cholbut SLN might be used in neoadjuvant chemotherapy, allowing potentially curative surgery, or after surgical resection to inhibit local relapses and metastasis development.

Inflammation is present in most cancer tissues, including those that have no precancerous lesions, and a constant inflammatory state may be necessary to maintain and promote cancer progression to a fully malignant phenotype by supporting tumor remodelling, neoangiogenesis, metastasis dissemination, and even modulation of the anticancer innate immune response from a protective M1-type response to a tumor-promoting M2-type response (Wang *et al*., 2009). Accordingly, the previously reported anti-inflammatory activity of cholbut SLN (Dianzani et al., 2006), may add value to the anti-cancer activity of this compound since it might help to reset the innate immune response. Since SCID mice display a severe defect of the adaptive immune response but maintain a weak innate immune response (Moser *et al*., 1993; Thomsen *et al*., 2008), this anti-inflammatory effect might have had a role in our in vivo experiments.

In conclusion, cholbut SLN seems to be an effective delivery system for cholbut because it decreases the active compound concentration, tumor refractoriness and toxic effects, and expands the

compound's mechanisms of actions, enabling it to act on multiple key fronts of anti-tumor activity, such as tumor cell growth, adhesion, and migration, and recruitment of inflammatory cells.

ACKNOWLEDGEMENTS

This research has been supported by Associazione Italiana Ricerca sul Cancro (AIRC, Milan), Regione Piemonte (Piattaforme Innovative - IMMONC, Converging Technologies NANO-IGT , Fondazione Amici di Jean (Turin), PRIN Project 2009 (MIUR, Roma) and Progetti di Ricerca di Ateneo San Paolo 2011.

CONFLICT OF INTEREST

P Gasco is an employee of Nanovector s.r.l.

REFERENCES

Asano T, Yao Y, Zhu J, Li D, Abbruzzese JL, Reddy SA (2004). The PI 3-kinase/Akt signaling pathway is activated due to aberrant Pten expression and targets transcription factors NF-kappaB and c-Myc in pancreatic cancer cells. Oncogene 23: 8571– 8580.

Brioschi A, Zara GP, Calderoni S, Gasco MR, Mauro A (2008). Cholesterylbutyrate solid lipid nanoparticles as a butyric acid prodrug. Molecules 13: 230-254.

Davis ME, Chen ZG, Shin DM (2008). Nanoparticle therapeutics: an emerging treatment modality for cancer. Nat Rev Drug Discov 7: 771-782.

Delzenne N, Cherbut C, Neyrinck A (2003). Prebiotics: actual and potential effect in inflammatory and malignant colonic disease. Curr Opin Clin Nutr Metab Care 6: 581-586.

Dianzani C, Cavalli R, Zara GP, Gallicchio M, Lombardi G, Gasco MR *et al.* (2006). Cholesteryl butyrate solid lipid nanoparticles inhibit adhesion of human neutrophils to endothelial cells. Br J Pharmacol 148: 648-656.

Dianzani C, Minelli R, Mesturini R, Chiocchetti A, Barrera G, Boscolo S *et al.* (2010). B7h triggering inhibits umbelical vascular endothelial cell adhesiveness to tumor cell lines and polymorphonuclear cells. J Immunol 185: 3970-3979.

Gasco MR (2004). Solid lipid nanospheres suitable to a fast internalization into cells. EP 1133286, (24/11/2004) – U.S. 6.685.960 (3/02/2004).

Hayot C, Debeir O, Van Ham P, Van Damme M, Kiss R, Decaestecker C (2006). Characterization of the activities of actin-affecting drugs on tumor cell migration. Appl Pharmacol 211: 30-40.

Itoh N, Semba S, Ito M, Takeda H, Kawata S, Yamakawa M (2002). Phosphorylation of Akt/PKB is required for suppression of cancer cell apoptosis and tumor progression in human colorectal carcinoma. Cancer 94: 3127–3134.

Iwahshi T, Okochi E. Ono K. Sugawara I, Tsuruo T, Mori S (1991). Establishment of multidrug resistant human colorectal carcinoma HCT-15 cell lines and their properties. Anticancer Res 11: 1309-12.

Khaleghpour K, Li Y, Banville D, Yu Z, Shen SH (2004). Involvement of the PI 3-kinase signaling pathway in progression of colon adenocarcinoma. Carcinogenesis 25: 241–248.

Kobayashi H, Tan EM, Fleming SE (2003). Sodium Butyrate Inhibits Cell Growth and Stimulates p21WAF1/CIP1 Protein in Human Colonic Adenocarcinoma Cells Independently of p53 Status. Nutr Cancer 46**:** 202-211.

Kwiatkowska A, Kijewska M, Lipko M, Hibner U, Kaminska B (2011). Downregulation of Akt and FAK phosphorylation reduces invasion of glioblastoma cells by impairment of MT1-MMP shuttling to lamellipodia and downregulates MMPs expression. Biochim Biophys Acta. 1813: 655-67.

Lai KC, Huang AC, Hsu SC, Kuo CL, Yang JS, Wu SH, Chung JG (2010). Benzyl isothiocyanate (BITC) inhibits migration and invasion of human colon cancer HT29 cells by inhibiting matrix metalloproteinase-2/-9 and urokinase plasminogen (uPA) through PKC and MAPK signaling pathway. J Agric Food Chem 58: 2935-42.

Lee J, Kim SJ, Choi H, Kim YH, Lim IT, Yang HM, Lee CS, Kang HR, Ahn SK, Moon SK, Kim DH,Lee S, Choi NS, Lee KJ (2010). Identification of CKD-516: a potent tubulin polymerization

inhibitor with marked antitumor activity against murine and human solid tumors. J Med Chem. 53: 6337-54.

Li B, Sun A, Youn H, Hong Y, Terranova PF, Thrasher JB, Xu P (2007). Conditional Akt activation promotes androgen-independent progression of prostate cancer. Carcinogenesis 28: 572–583.

Loberg RD, Day LL, Dunn R, Kalikin LM, Pienta KJ (2006). Inhibition of decay-accelerating factor (CD55) attenuates prostate cancer growth and survival in vivo. Neoplasia. 8(1):69-78.

Matsumura Y, Kataoka K (2009). Preclinical and clinical studies of anticancer agent-incorporating polymer micelles. Cancer Sci 100: 572-579.

Matsuoka T, Yashiro M, Nishioka N, Hirakawa K, Olden K, Roberts JD (2012). PI3K/Akt signalling is required for the attachment and spreading, and growth in vivo of metastatic scirrhous gastric carcinoma. Br J Cancer 106: 1535-42.

Minelli R, Serpe L, Pettazzoni P, Minero V, Barrera G, Gigliotti C, Mesturini R, Rosa A, Gasco P, Vivenza N, Muntoni E, Fantozzi R, Dianzani U, Zara G, Dianzani C (2012). Cholesteryl butyrate solid lipid nanoparticles inhibit the adhesion and migration of colon cancer cells. Br J Pharmacol 166:587-601.

Minucci S, Pelicci PG (2006). Histone deacetylase inhibitors and the promise of epigenetic (and more) treatments for cancer. Nat Rev Cancer 6: 38–51.

Mosier DE, Stell KL, Gulizia RJ, Torbett BE, Gilmore GL (1993). Homozygous scid/scid;beige/beige Mice Have Low Levels of Spontaneous or Neonatal T Cell-induced B Cell Generation. J Exp Med 177: 191-194

Pellizzaro C, Coradini D, Morel S, Ugazio E, Gasco MR, Daidone MG (1999). Cholesteryl butyrate in solid lipid nanospheres as an alternative approach for butyric acid delivery. Anticancer Res 19: 3921–3926.

Roy HK, Olusola BF, Clemens DL, Karolski WJ, Ratashak A, Lynch HT, Smyrk TC (2002). Akt proto-oncogene overexpression is an early event during sporadic colon carcinogenesis. Carcinogenesis 23: 201–205.

Salomone B, Ponti R, Gasco MR, Ugazio E, Quaglino P, Osella-Abate S *et al.* (2001). In vitro effects of cholesteryl butyrate solid lipd nanospheres as a butyric acid prodrug on melanoma cells: evaluation of antiproliferative activity and apoptosis induction. Clinic. Experim. Metast 18: 663–673.

Serpe L, Laurora S, Pizzimenti S, Ugazio E, Ponti R, Canaparo R *et al.* (2004). Cholesteryl butyrate solid lipid nanoparticles as a butyric acid pro-drug: effects on cell proliferation, cell cycle distribution and c-myc expression in human leukemic cells. Anti Cancer Drugs 15: 525–536.

Shukla S, Maclennan GT, Hartman DJ, Fu P, Resnick MI, Gupta S (2007). Activation of PI3K-Akt signaling pathway promotes prostate cancer cell invasion. Int J Cancer 121: 1424-32.

Stein U, Walther W, Shoemaker RH (1996). Reversal of multidrug resistance by transduction of cytokine genes into human colon carcinoma cells. J Natl Cancer Inst 88: 1383-92.

Singh R, Lillard JW Jr (2009). Nanoparticle-based targeted drug delivery. Exp Mol Pathol 86: 215-23.

Thomsen M, Galvani S, Canivet C, Kamar N, Böler T. (2008). Reconstitution of immunodeficient SCID/beige mice with human cells: Applications in preclinical studies.
Toxicology 246: 18-23.

Wang F, Arun P, Friedman J, Chen Z, Van Waes C (2009). Current and potential inflammation targeted therapies in head and neck cancer. Curr Opin Pharmacol 9; 389-395.

Wilson AJ, Chueh AC, Tögel L, Corner GA, Ahmed N, Goel S, Byun DS, Nasser S, Houston MA, Jhawer M, Smartt HJ, Murray LB,Nicholas C, Heerdt BG, Arango D, Augenlicht LH, Mariadason JM (2010). Apoptotic sensitivity of colon cancer cells to histone deacetylase inhibitors is mediated by an Sp1/Sp3-activated transcriptional program involving immediate-early gene induction. Cancer Res

70: 609-20.

Wollowski I, Rechkemmer G, Pool-Zobel BL (2001). Protective role of probiotics and prebiotics in colon cancer. Am J Clin Nutr. 73: 451S-455S.

Wong HL, Bendayan R, Rauth AM, Li Y, Wu XY (2007). Chemotherapy with anticancer drugs encapsulated in solid lipid nanoparticles. Adv Drug Deliv Rev 59: 491-504.

Wu C, Huang J (2007). PI3 kinase-Akt-mTOR pathway is essential for neuroendocrine differentiation of prostate cancer J Biol Chem 282: 3571-3583.

LEGENDS

Figure 1. *Laser Doppler Micro-electrophoresis analysis (LDME).* The test was performed on cholbut SLN using a Malvern Zetasizer – Nano ZS. Results are showed as total count on Zeta Potential (mV).

Figure 2. *Field Emission Scanning Electron Microscopy (FeSEM) analysis.* Image shows the morphology of cholbut SLN. White bars represent as scale unite of 200 nm (by cooperation with Polytechnik of Turin)

Figure 3. *Inhibition of proliferation following cholbut SLN and NaBut treatment.* Cells (800/well) were treated with increasing concentrations (50 - 300 μM) of cholbut SLN and NaBut for 24-72 h and the result was expressed as the percentage of inhibition versus the control expressed as mean ± SEM (n=5). In some experiments, cholbut SLN and NaBut were refilled every 24 h (n=5) without changing the culture medium (48h culture: 24+24h; 72 h culture: 24+24+24h). One-way ANOVA and the Dunnett's test revealed statistically significance differences (* $p<0.05$; ** $p<0.01$) of treated versus control cells. The experiments were performed on HT29 (A), HCT116 (B), HCT15 (C), and PC-3 (D) cells.

Figure 4. *Effect of cholbut SLN and NaBut on cell clonogenicity was tested by colony forming assay.* **A:** HT29, HCT116, HCT15 and PC-3 cells (500/well) were seeded in 6 well plates and treated with each drug at the indicated concentrations for 72 hours. The medium was then changed and cells were cultured for additional 10 days and subsequently fixed and stained with crystal violet (n=5). **B:** Quantification of the percentage of inhibition versus the control. Data were analyzed by the one-way ANOVA and the Dunnett's tests (* $p<0.05$; ** $p<0.01$ versus the control).

Figure 5. *Induction of cell cycle arrest by cholbut SLN treatment.* A-B: PC-3 cells ($1.5x10^5$) were treated or not with 50 µM-0.3 mM cholbut SLN for 24-72 h and cell cycle was then assessed by flow cytmetry. **C-D:** in these experiments, 50 - 300 µM cholbut SLN was refilled every 24 h (48h colture: 24+24h; 72 h culture: 24+24+24h) without changing the culture medium (A and C: representative cell cycle plots; B and D**:** quantification of cell cycle phases; n=3).

Figure 6. *Induction of cell death following treatment with cholbut SLN.* PC-3 cells ($1.5x10^5$) were treated or not with 50 - 300 µM cholbut SLN refilling for 48 (24+24h) -72 h (24+24+24 h) and cell death was then assessed by flow cytometry (n=3). One-way ANOVA and the Dunnett's test revealed statistically significance differences (* $p<0.05$; ** $p<0.01$) of treated versus control cells.

Figure 7. *Effect of cholbut SLN on Akt phosphorylation in HCT15 (**A**), HCT116 (**B**), HT29 (**C**) and PC-3 (**D**).* Cells were treated with 100 µM cholbut SLN for 8, 24 or 48 h and subsequently incubated with fresh media containing (0.01 µM) PMA to induce Akt phosphorylation, which was then evaluated by Western blot in the cell lysates; the same blots were probed with anti β-actin antibody as a control. **Left**: Western blot analysis from a representative experiment. **Right**: Densitometric analysis of Akt phosphorylation expressed in arbitrary units from three independent experiments. Data are expressed as mean±SEM (n=3) of the percentage of inhibition versus the control. Data were analyzed by the one-way ANOVA and the Dunnett's tests (** $p<0.01$ versus the control).

Figure 8. *Effect of cholbut SLN on tumor cell dissemination in vivo.* Mice were injected i.v. with $1x10^6$ PC-3-Luc cells and treated with 220 $mM \cdot Kg^{-1}$ cholbut SLN (n=5) or PBS (control group, n=4). **A:** At time 0, and 7, 14, and 21 days after cell injection, mice were i.p. injected with luciferin and pulmonary metastases were macroscopically detectable and documented by *in vivo* optical imaging. **B:** The luminescent signal was quantified as the average radiance ($p/s/cm^2/sr$) measured in regions of interest (ROIs) drawn in lungs. **C**: Non-sequential serial sections were taken from lungs of animals and stained with hematoxylin/eosin to highlight pulmonary metastasis. Representative histological analysis of the lungs in control mice (**left panel**) and in treated mice (**right panel**).
Statistical analysis was performed with the one-way ANOVA and the Dunnett's tests (** $p<0.01$, *** $p<0.001$ versus the control).

Figure 9. *Effect of cholbut SLN on local tumor growth in vivo*. Mice were injected s.c. with PC-3 cells

and treated with either 220 $mM \cdot Kg^{-1}$ cholbut SLN (n=4) or PBS (control group, n=3) starting when the tumor diameter reached 2 mm^3 (size of sc tumors was weekly measured by calipers). Statistical analysis was performed with the one-way ANOVA and the Dunnett's tests (** $p<0.01$, *** $p<0.001$ versus the control).

Table 1. *DLS analysis (Malvern Zetasizer – Nano ZS)* Size distribution by intensity and polydispersity index . Characterization of cholbut SLN at different steps of the preparation.

Cholbut SLN	Zave (nm)	Poly dispersity Index (PI)
Before washing	87,72	0,235
After washing (n=4)	79,83	0,254
After sterilizing filtration (0,2µm)	78,48	0,248

Table 1

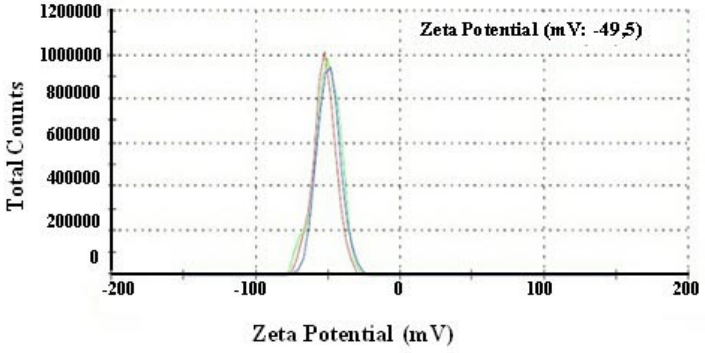

Figure 1

Figure 1.TIF

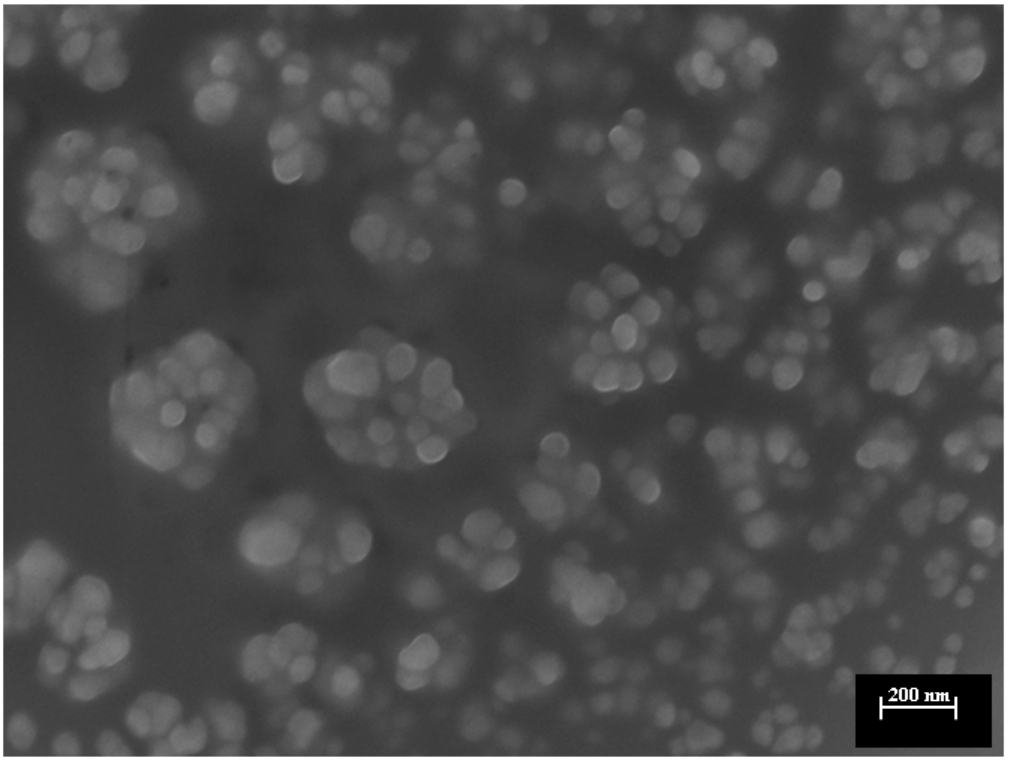

Figure 2

Figure 2.TIF

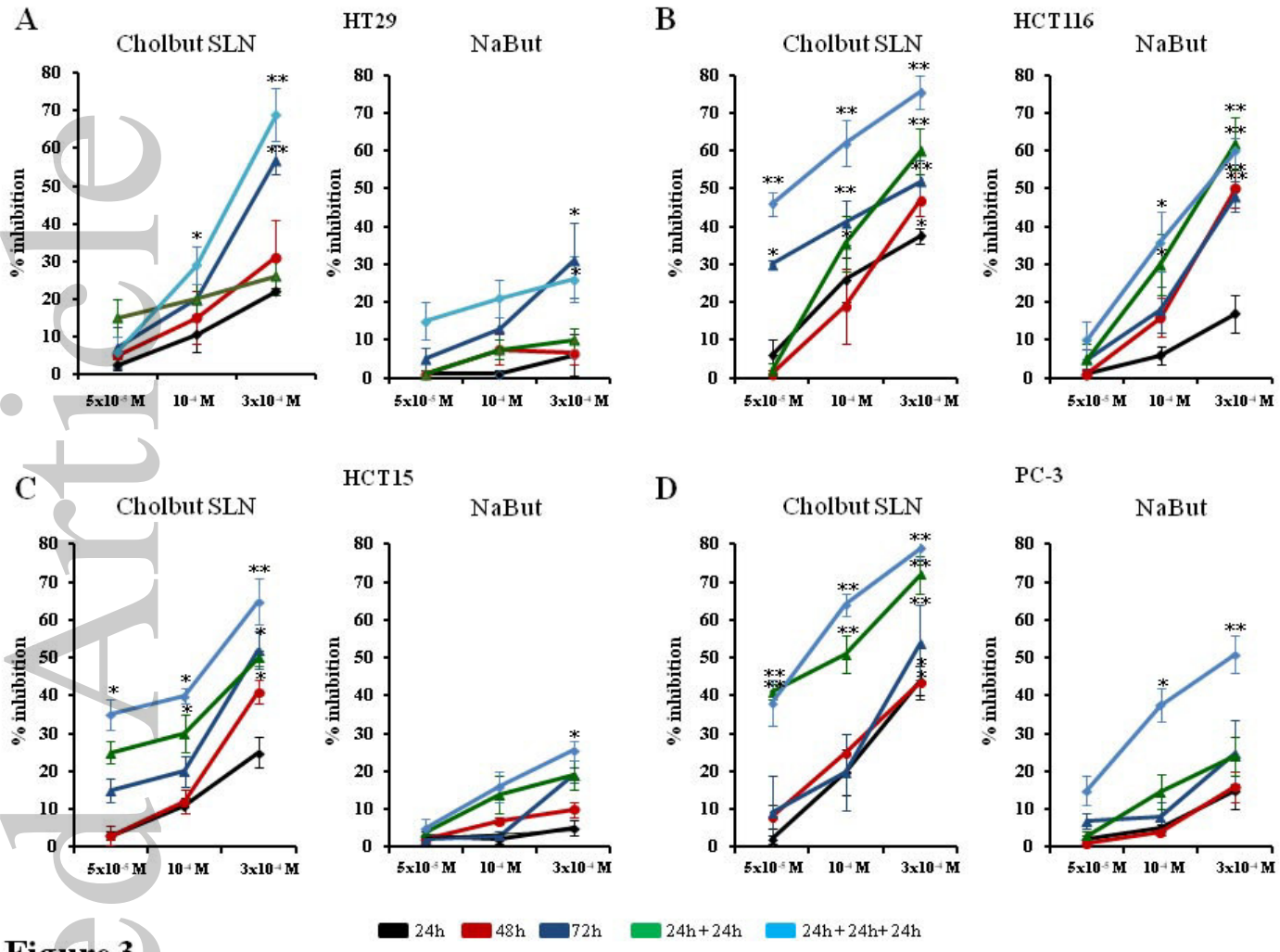

Figure 3

Figure 3.TIF

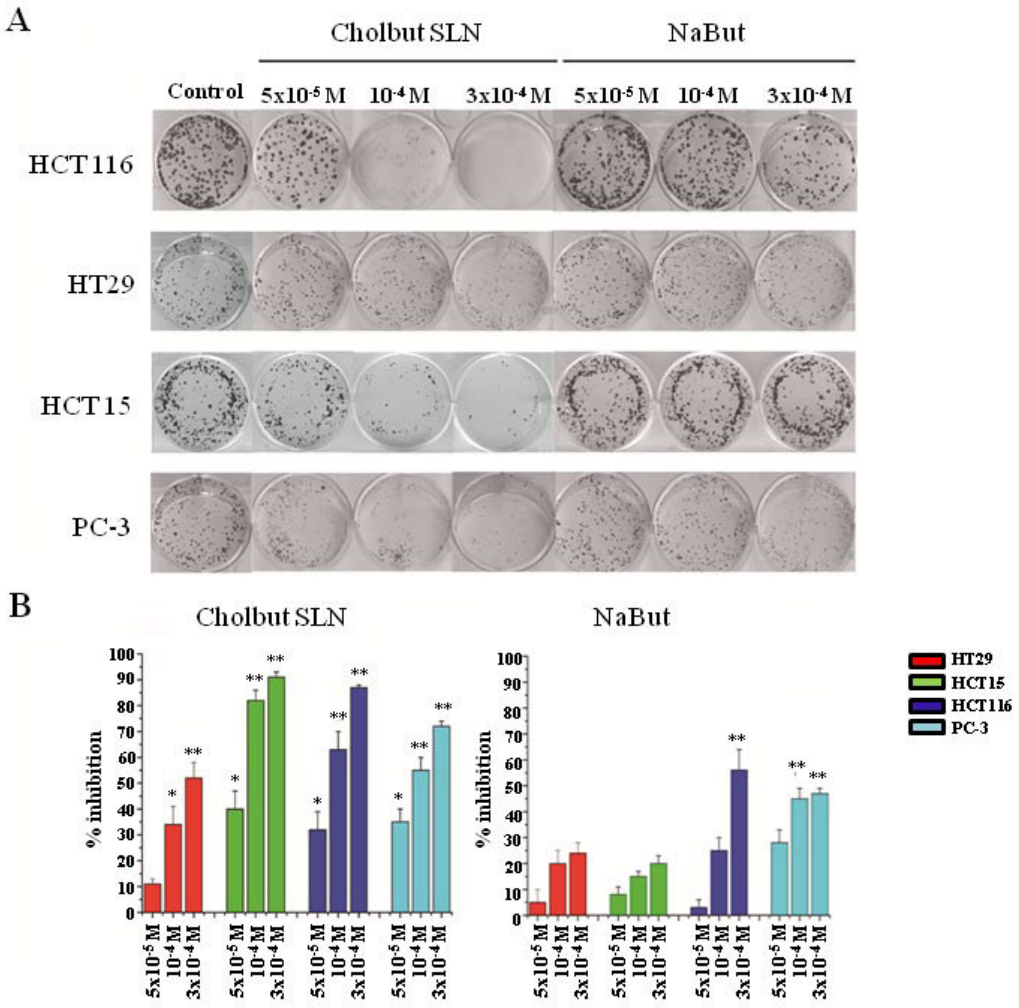

Figure 4

Figure 4.TIF

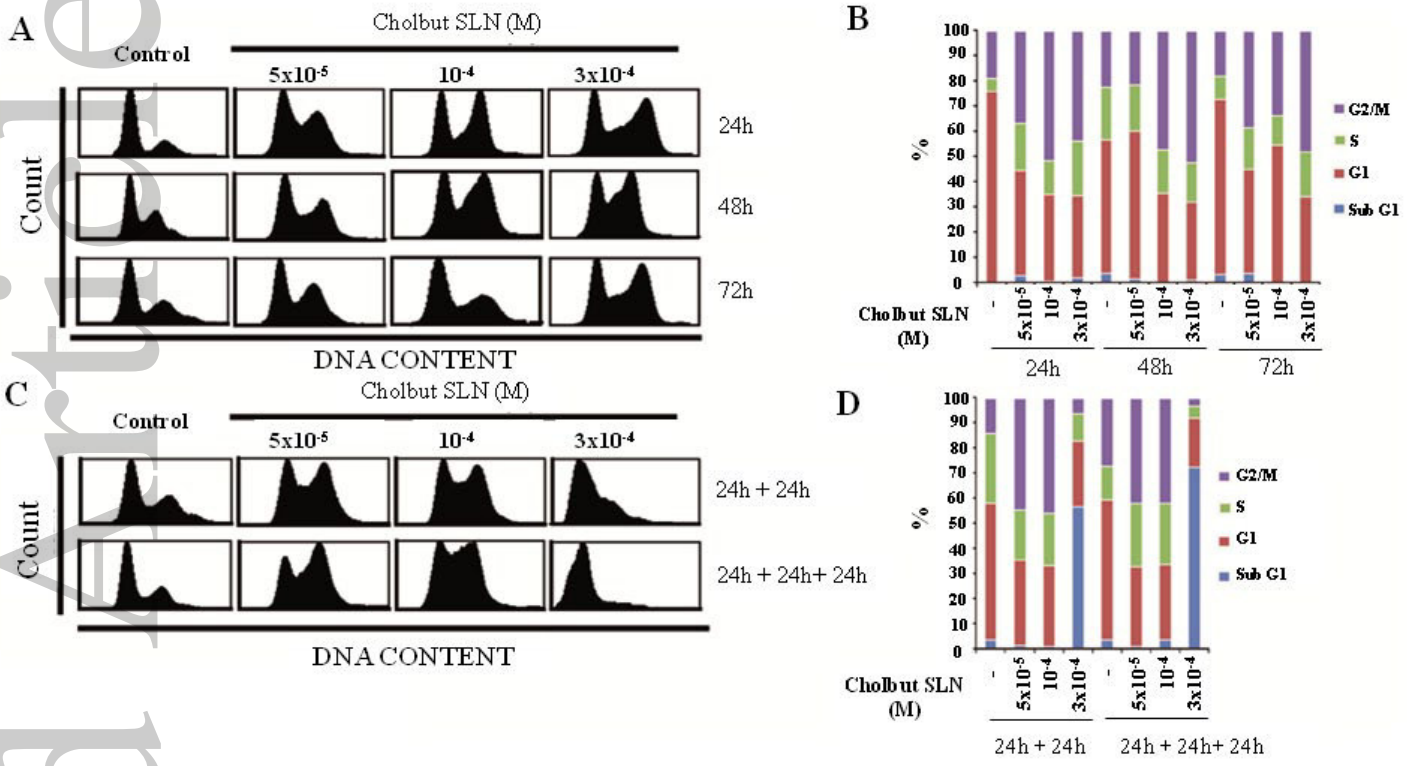

Figure 5

Figure 5.TIF

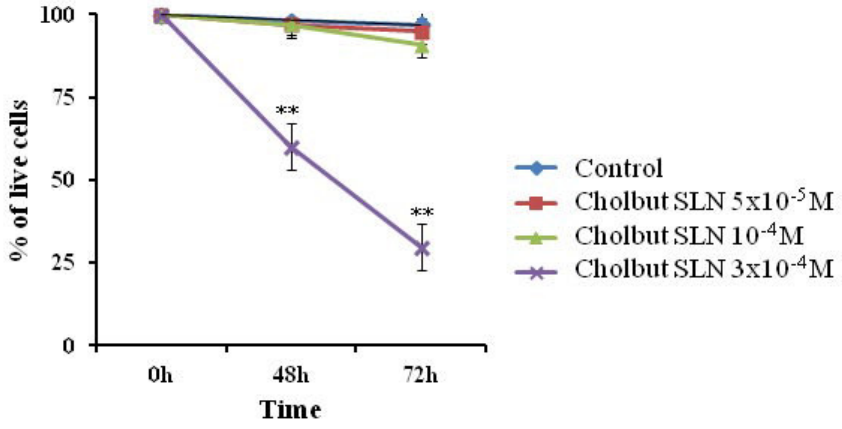

Figure 6

Figure 6.TIF

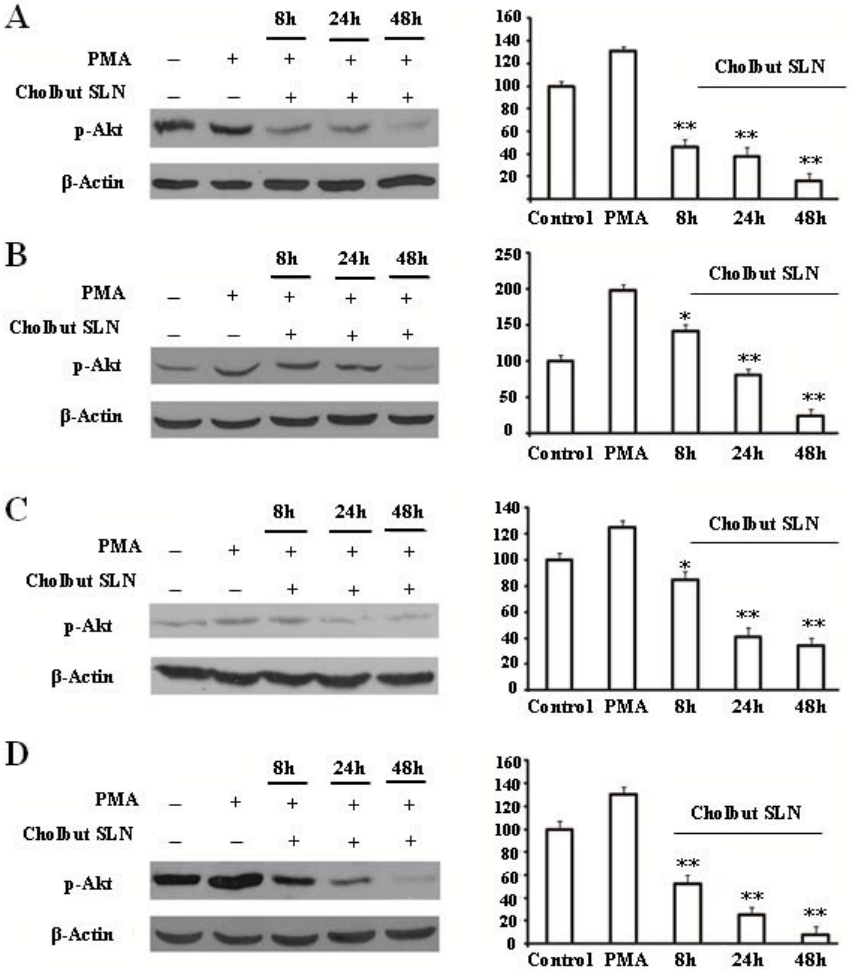

Figure 7

Figure 7.TIF

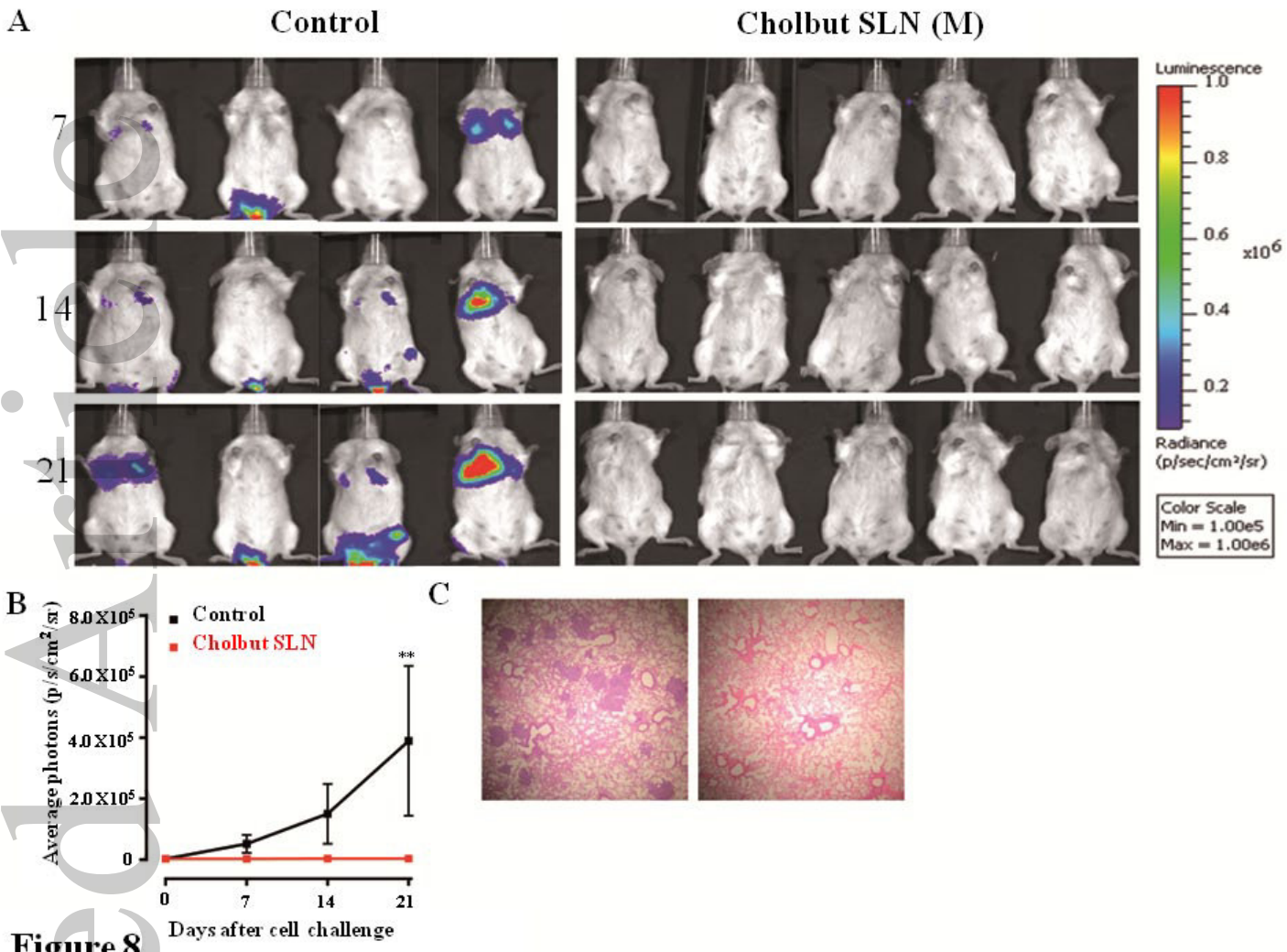

Figure 8

Figure 8.TIF

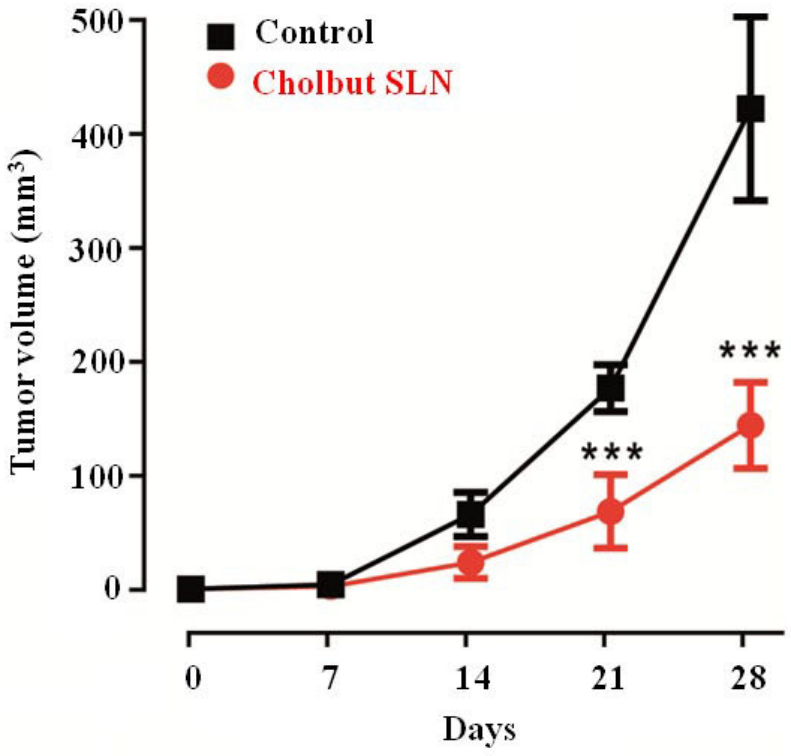

Figure 9

Figure 9.TIF